Equation of state and transport properties of an interacting multispecies plasma: Application to a multiply ionized Al plasma

F. Perrot
Centre d'Etudes de Limeil-Valenton, 94195 Villeneuve-St.-Georges Cedex, France

M. W. C. Dharma-wardana
National Research Council, Ottawa, Canada K1A 0R6

(Received 28 November 1994; revised manuscript received 24 April 1995)

We present a first-principles theory of the ionization equilibrium, thermodynamics, and linear transport properties of an interacting mixture of electrons and several species of ions and neutral atoms, typical of a hot plasma. The thermodynamic functions are self-consistently calculated using the density functional theory (DFT). The inputs are the nuclear charge Z, the average electron density $\overline{n}$, the temperature T, and the configurations of the ions and neutral atoms to be considered. Ion-electron pseudopotentials and ion-ion pair potentials (including repulsive core contributions) are derived from the DFT. The ionic structure factors are determined using the multicomponent hypernetted chain theory. The ion-species concentrations x_i are obtained through a minimization of the total free energy F at constant volume and temperature. The average ionization Z^*, the internal energy, the pressure, and the resistivity are computed. The method is illustrated by applications to aluminum plasma. In the calculations for expanded Al at $T = 1.5$ eV we find a low electron-density range where two solutions are obtained for a given average atomic volume; the most stable has the highest ionization. The unstable solution has an excitation energy that can reach 2.5 eV. At a higher density, the results imply a *plasma phase transition* from a state with average ionization $Z^*=1.2$ to a state with $Z^*=3$. We also provide calculations for a variety of expanded, compressed, and shocked plasmas, which are of current theoretical and experimental interest.

PACS number(s): 52.25.Kn, 61.25.Mv, 64.30.+t, 65.50.+m

I. INTRODUCTION

The average ionization Z^* is a fundamental quantity entering most theories of liquid metals or plasmas and is directly related to the "free" electron density $\overline{n}$ in the plasma. Some physical properties depend crucially on Z^*. Typical examples of such properties are the plasma pressure and the electrical and thermal conductivities. The dynamic analogs of the conductivities (e.g., photoabsorption cross sections) also involve Z^* and relaxation times closely related to those in the static conductivities. Many experiments for probing plasmas depend on measurements of the static and dynamic conductivities [1–3]. Such transport measurements could also be an indicator of phase transitions in plasmas [4] and in metallic vapors [5]. The ionization balance and the equation of state (EOS) are also of great importance in astrophysical studies [6,7]. Saha theory [8] can be used to calculate the EOS and the associated ionization balance in low density plasmas. Saha theory treats the thermal equilibrium between various ideal, "isolated" atomic and ionic or molecular species, essentially in the ground state, and an unperturbed uniform noninteracting electron gas. The modifications in the electronic structure induced by matter density, temperature, interactions between the ions, etc., are not taken into account in this theory, which is restricted to very low densities and temperatures. However, real low density systems are characterized by molecule formation, large density fluctuations etc., and Saha theory is in practice inapplicable. Even the "ideal" low density theory needs to address the divergencies in the partition functions of isolated atoms by appealing to other considerations [9] before Saha theory can be implemented [10]. While quantum cluster expansion methods [11] can in principle be applied to take account of "nonideal" behavior, such methods, based on expansions about the ideal limit, tend to be extremely inconvenient in practice, even for moderate densities, and an adequate treatment of electron-electron and electron-ions interactions remains an open problem. Thus other approaches [12,13] to the equation of state of ion-electron systems have been developed over the years, where intuitively reasonably but somewhat *ad hoc* assumptions are used to deal with Coulomb interactions, bound states, and hard repulsive cores at each ion and to smoothen the discontinuities in including the bound and continuum contributions to the partition function.

Another approach to the calculation of the EOS is provided by self-consistent calculations of average atoms [14–16], which have become very popular in EOS and opacity calculations. Models of average atoms in plasmas may be either restricted to a single "ion sphere" or adapted to an atom in an infinite medium, but they are always solved in spherical symmetry. The plasma environment is in general modeled either by an infinite jellium

or by appropriate boundary conditions on the "atomic sphere." Two important consequences result from these approximations.

(i) The multicenter structure is not treated explicitly. An easily tractable refinement is to build up the total electron charge density as a superposition of single charge densities, as done in the theory of simple metals. But this is not suitable when the density and temperature conditions are such that the energy gap between the conduction band and the outermost bound level approaches zero. In such cases, an abrupt change in ionization, and consequently in resistivity, is found. Such abrupt changes can occur if there is a real phase transition in the system and hence the theory must be free of model-dependent artifacts to make confident predictions.

(ii) The multispecies effects on ion equilibria and transport are neglected, Z^* being determined from the spectrum and wave functions of a single "average" ion.

In this work, we *retain the first approximation of using single-center methods* and work in an appropriate regime of density and temperature to address the second issue and show how to include the interactions between ions, as in simple (single-center) liquid theory, in the calculation of ionization by explicitly including the relevant ionic species present in the plasma. The equilibrium among these species results from the minimization of the total free energy of the system. All the ingredients of the model are calculated *a priori*; the energies of the various species are self-consistently determined for ions embedded in the appropriate electron environment, the pair interactions are deduced from the electronic structure of these ions and the pair correlation functions are obtained by solving the coupled hypernetted chain equations. The formulation begins from the system Hamiltonian and the approximations made at each step can be clearly indicated.

The paper is organized as follows. In Sec. II we present the theory of an interacting multispecies model and explain how the quantities entering the equilibrium equations are calculated. Applications to Al plasmas at several densities and temperatures are presented and compared with average atom calculations using a single average-structure model. A detailed account of the Al plasma at a temperature of 1.5 eV is reported in Sec. III, where a transition between an ionized phase with $Z^* \simeq 1.2$ and the $Z^* = 3$ phase, characteristic of a "plasma phase transition," is predicted to occur in a rather small range of compressions 0.27–0.40. An unstable phase with a weak ionization around $Z^* = 0.1$ is found. We also report more wide ranging results of the ionization Z^* and the electrical resistivity R of expanded and compressed plasmas and along the principal shock Hugoniot curve, using the appropriate theory in each density and temperature range. These results are useful in the design of experiments and for comparison with other methods that use more drastic simplifications or non-first-principles parametrizations to achieve easy "on line" computability. Finally, concluding remarks and an assessment of the approximations made in the present method are given in the Conclusion, while technical issues are dealt with in Appendixes A–C.

II. THEORY OF DENSITY EFFECTS AND ION-ION INTERACTIONS

The temperature T, the nuclear charge Z, and an average electron density $\overline{n}$ are chosen as the input quantities characterizing the plasma. The case of several elements having different nuclear charges brings no difficulty, but is dropped for simplicity. The temperature T is higher than the critical temperature to prevent transition to the gaseous neutral phase. Several ionic species, having charge states Z_i, are present in non-negligible concentrations x_i in this plasma. There is no formal complication in including clusters (i.e., multicenter objects) in the theory given here. As cluster calculations in plasmas require multicenter numerical methods, we limit ourselves to plasmas such that *single-center* methods are sufficient. The single-center assumption is consistent with the assumption of integral charge states $Z_i = 0, 1, 2, \ldots$ for the basic configurations assumed in this paper. If chemical bonding (molecule formation) is allowed, charge can reside in the midbond region and integral charge states cannot be used as a basis for describing the atomic configurations. In Sec. III B we discuss the condition for molecule formation and restrict the regime of application of our calculations to *ensure that our assumptions hold.* Thus we consider only simple ionic species, e.g., Al^{z_i+}, where the ionic charge Z_i could be 0, 1, 2, 3, ... The calculation of pair potentials is formally equivalent to the calculation of binary clusters. In the present work this is achieved in second-order perturbation theory with the help of pseudopotentials, thus avoiding the full treatment of two-center systems.

A. Total free energy of the plasma

In calculating the free energy of the electron-nuclei mixture we proceed via the neutral-pseudoatom (NPA) model already discussed in the literature [17–19]. The total Hamiltonian of the system is initially written as $H = H_e + H_N + H_{Ne}$, with $H_e = H_e^0 + H_{ee}$ and $H_N = H_N^0 + H_{NN}$ being the contributions from the electron and nuclear subsystems. The electron-nuclear interaction H_{Ne} produces bound electronic states attached to each nucleus to form ions with effective charge Z_i. In studying simple plasmas, i.e., systems where the bound states are compactly associated with a single center, we can at this stage rewrite the Hamiltonian using a description in terms of ions instead of bare nuclei. If the system is in a plasma (metallic) state, there is also a distribution of "continuum" electrons, with an average density $\overline{n}$. The Hamiltonian can be rewritten to explicitly bring out a uniform electron gas term H_{eg} by adding and subtracting a uniform density term to the total Hamiltonian and rearranging it [20]. The uniform neutralizing background term introduced at this stage is once again rearranged in replacing the "ions" by "pseudoions," which are weak scatterers by construction. That is, the electron-ion term in the Hamiltonian is manipulated by adding (and subtracting from the total Hamiltonian) a spherical Wigner-Seitz cavity ν_i in the positive background around each

ionic center i. The ion, together with its cavity, forms a weak scatterer with a Friedel sum equal to zero and constitutes the NPA. Since this object is a weak scatterer by construction, perturbation theory can be applied to it. The construction of the NPA, with its bound and free electron distributions for each Z_i, requires the full nonlinear self-consistent scheme of the finite temperature density functional theory (DFT). The NPA approach assumes that the effect of the cavity that is added and subtracted can be treated by perturbation theory. When this is not possible (e.g., as in the case of hydrogen plasmas) a procedure involving coupled density functional equations (one for the ions, another for the electrons) is needed [16]. In the case of plasmas made up of "simple metallic ions," the assumptions of the NPA model hold very well for the ionization states usually encountered. For a chosen set of ionization states Z_i, the average ionization Z^*, the matter density ρ, the free electron density $\overline{n}$, and the ionic concentrations x_i are related by

$$Z^* = \sum_i x_i Z_i, \ \rho = \overline{n}/Z^*. \tag{1}$$

Thus, instead of starting from the matter density ρ, it is convenient to take $\overline{n}$ and T as the primary inputs to the calculation and determine x_i, Z^*, and ρ from the thermodynamics. We need the total free energy F as well as its derivatives $\delta F/\delta\overline{n}$, $\delta F/\delta T$, and $\delta F/\delta x_i$.

The total free energy per ion of the plasma is

$$F = F_{id} + F_{eg} + F_{em} + F_{xs}. \tag{2}$$

The first term F_{id} is the ideal ion-fluid contribution

$$F_{id} = -k_B T \left[\ln\{(2\pi MkT/h^2)^{3/2}\rho^{-1}e\} - \sum_i x_i \ln x_i \right]. \tag{3}$$

M is the nuclear mass, N is the total number of nuclei, and $x_i = N_i/N$ is the concentration of the ith ionic species. F_{eg} is the free energy of the interacting electron gas

$$F_{eg} = Z^* f(\overline{n}, T) = \Omega\overline{n} f(\overline{n}, T). \tag{4}$$

Z^* is the average number of free electrons per ion. Ω is the average atomic volume and $f(\overline{n}, T)$ is the uniform electron gas free energy [21] per electron at density $\overline{n}$ and temperature T. From the definition of the electron chemical potential μ, when the average density changes by an amount $\delta\overline{n}$ we have

$$\delta F_{eg} = \Omega\mu\delta\overline{n} = Z^*\mu\delta\overline{n}/\overline{n}. \tag{5}$$

We discuss $F_{\rm em}$, F_{xs}, viz., the embedding energy and the excess free energy in the following subsections.

The third contribution $F_{\rm em}$ to F [Eq. (2)] is the free energy required to "embed" the various kinds of ions in the electron gas. Explicitly, the embedding energy F_i of ion species i is defined as the free energy of the electron gas containing the ion of species i minus the free energy of the unperturbed electron gas but inclusive of certain corrections discussed below. The theory assumes that these ion-energy terms can be calculated independently of each other, i.e., $F_{\rm em}$ is a linear form $\sum_i x_i F_{i,\rm em}$. This implies that the bound electrons are those that are sufficiently rigid to fluctuations in the environment. Furthermore, the conduction-electron screening charge density is, as in a metal, taken as a superposition of the individual screening clouds of each ion. Thus each species is calculated self-consistently by solving the Mermin-Kohn-Sham equations [22] in an infinite jellium of density $\overline{n}$, for the nucleus surrounded by a cavity ν_i of volume $\Omega_i = Z_i/\overline{n}$ and radius R_i such that $4\pi R_i^3\overline{n}/3 = Z_i$. Thus

$$\nu_i(r) = \overline{n}[\theta(0) - \theta(r - R_i)]. \tag{6}$$

Here $\theta(x)$ is the Heaviside step function. The "nucleus plus cavity plus its electronic cloud" constitutes the NPA, which has been discussed in several contexts [17,18]. Such self-consistent calculations of the free energy and internal energy of an ion embedded in an electron gas surrounded by a cavity have been described in previous work [19,18]. The free energy of the NPA, calculated in the "external potential"

$$V_{{\rm ext},i}(r) = -Z_i/r + \nu_i(r') \otimes |\mathbf{r} - \mathbf{r}'|^{-1} \tag{7}$$

and in the presence of the electron gas is F_i. The symbol $\otimes$ means, as usual, integration in all space $\mathbf{r}'$. We do not reproduce here all the details of this standard calculation. However, we remark that we replace the noninteracting entropy of the bound "Kohn-Sham" electrons calculated in the DFT model, namely,

$$-k_B\,[n_q \ln(c_q) + (g_q - n_q)\ln(1 - c_q)], \ c_q = n_q/g_q \tag{8}$$

for shell q with degeneracy g_q and population n_q, by its exact form derived from the statistical weight for shell q:

$$k_B \ln[g_q!/\{n_q!(g_q - n_q)!\}]. \tag{9}$$

With this correction we obtain F_i defined as the free energy of the electron gas containing the ion minus the free energy of the unperturbed electron gas. To obtain the total embedding energy, one has to correct for the cavity surrounding the ion, as in Ref. [19]. We first define the total Coulomb potential $V_i(r)$ associated with the ion i. If $\Delta n_i(r)$ is the total *displaced* electron charge distribution resulting from the self-consistent DFT calculation for the ion of species i in the external potential $V_{{\rm ext},i}$, then

$$V_i(r) = -Z_i/r + [\nu_i(r') + \Delta n_i(r)] \otimes |\mathbf{r} - \mathbf{r}'|^{-1}. \tag{10}$$

The cavity $\nu_i(r)$ around each ion implies a charge deficit $\eta_i(r) = \overline{n} - \nu_i(r)$. Thus the cavity correction L_i, which has to be added to F_i, is now easily shown to be

$$L_i = \eta_i(r) \otimes V_i(r) - \frac{1}{2}\eta_i(r) \otimes \frac{1}{|\mathbf{r} - \mathbf{r}'|} \otimes [\nu_i(r') - m_i(r')]. \tag{11}$$

Here $m_i(r)$ is the electron density displacement due

to the cavity ν_i and is of the form $m_i(q) = -\nu_i(q)v(q)\Pi(q,\overline{n})$, with $v(q) = 4\pi/q^2$ and $\Pi(q,\overline{n})$ the interacting electron gas response function at the density $\overline{n}$. Hence, finally,

$$F_{\rm em} = \sum_i x_i F_{i,\rm em} = \sum_i x_i (F_i + L_i). \tag{12}$$

In calculating $\delta F_i/\delta\overline{n}$ we define $f_i = \overline{n}\delta F_i/\delta\overline{n}$ and the Mermin-Kohn-Sham variational property yields

$$f_i = -\eta_i(r) \otimes V_i(r) - Z_i V_i(R_i). \tag{13}$$

We also define $l_i = \overline{n}\delta L_i/\delta\overline{n}$ for variations arising from the cavity correction. An explicit form for l_i is given in Appendix A. Hence, finally, we have

$$\delta F_{\rm em} = \sum_i x_i (f_i + l_i)\delta\overline{n}/\overline{n}. \tag{14}$$

The quantity $(f_i + l_i)$ is the *embedding contribution to the electron chemical potential* μ.

B. Excess free energy of the fluid

The displaced electron density $\Delta n_i(r)$ around the ion of species i referred to in Eq. (10) includes a bound contribution $n_{b,i}(r)$ and a continuum (free) contribution $\Delta n_{f,i}(r)$. We have shown in previous papers [23] how to extract pseudopotentials $w_i(q)$ that, by construction, reproduce the full *nonlinear* self-consistent free density $\Delta n_{f,i}(r)$ in *linear* response theory. This method works for ions that have the character of simple metallic ions, but it is not suitable for H^+ or for transition metal ions. The pseudopotentials may be used to construct the metallic part of the pair interactions between the ions

$$\phi_{ij}(r) = (2\pi)^{-3} \int \Pi(q,\overline{n}) w_i(q) w_j(q) \exp(i\mathbf{q}\cdot\mathbf{r}) d\mathbf{q}, \tag{15}$$

where $\Pi(q,\overline{n})$ is the finite-temperature interacting electron response function. A repulsive contribution φ_{ij} described in Appendix B must be added to the metallic contribution to obtain the total pair interaction

$$\psi_{ij} = \phi_{ij} + \varphi_{ij}. \tag{16}$$

A contribution to the pair potential due to core polarization effects can also be added [24], but this is not important in the plasmas considered here. The ionic structure of the fluid is then calculated by solving suitable coupled integral equations, e.g., hypernetted chain (HNC) equations modified to include bridge terms where necessary. The simple HNC scheme is sufficient for the plasmas considered here and has the advantage of not needing a coupling constant integration to obtain the free energy. The pair interaction free energy F_{xs}, often called the "excess free energy," is given in the coupled HNC scheme by [25]

$$F_{xs} = \sum_{i,j} x_i x_j F_{ij} - \frac{1}{2\beta\rho} \int \mathbf{F}(q;\rho) d\mathbf{q}, \tag{17}$$

with $\beta = 1/k_B T$ and

$$F_{ij} = \frac{\rho}{2\beta} \int d\mathbf{r} [g_{ij}(\ln g_{ij} + \beta\psi_{ij}) - h_{ij}(1 + \tfrac{1}{2}h_{ij})], \tag{18}$$

$$\mathbf{F}(q;\rho) = (2\pi)^{-3}\{\ln\det[\mathbf{I} + \rho\mathbf{H}] - \mathrm{Tr}[\rho\mathbf{H}]\}. \tag{19}$$

Here $\mathbf{I}$ is the unit matrix and $\mathbf{H}$ has elements $H_{ij} = \sqrt{x_i}\, h_{ij} \sqrt{x_j}$, where $h_{ij} = g_{ij} - 1$ involves the pair distribution function g_{ij} between the ionic species i and j.

The excess free energy F_{xs} is stationary with respect to all the h_{ij} at constant ρ and x_i. If a change is made in $\overline{n}$, the resulting change in F_{xs} comes only from the changes in ψ_{ij}. As the core-core repulsion φ_{ij} is very rigid (i.e., it is assumed to be insensitive to small changes in the ion environment or in $\overline{n}$), only ϕ_{ij} has to be considered. From the definition of F_{ij} [Eq. (18)] and ϕ_{ij} [Eq. (15)], it is clear that one can write for a change $\delta\overline{n}$

$$\delta F_{xs} = \sum_{ij} x_i x_j f_{ij} (\delta\overline{n}/\overline{n}), \tag{20}$$

with

$$f_{ij} = \frac{\rho}{2(2\pi)^3} \int d\mathbf{r} g_{ij} \int d\mathbf{q} \frac{\partial\Pi(q;\overline{n})}{\partial\overline{n}} w_i(q) w_j(q) \times \exp(i\mathbf{q}\cdot\mathbf{r}). \tag{21}$$

The temperature dependence of the response function is not written for simplicity. The density dependence of the pseudopotentials is weak enough to be neglected in the calculation of f_{ij}. The quantities f_{ij} are *corrections to the electron chemical potential arising from ion-ion interaction effects.*

C. Minimization of the free energy

The total free energy F of the system must be minimized with respect to the concentrations x_i, at constant volume Ω (or matter density ρ). The input quantity in our calculations is not the matter density ρ, but the electron density $\overline{n}$. The relation between these densities is given in Eq. (1). Hence the constraint $\delta\rho = 0$ reads

$$Z^* \frac{\delta\overline{n}}{\overline{n}} - \sum_i Z_i \delta x_i = 0. \tag{22}$$

Since $\sum_i x_i = 1$, we also have the constraint

$$\sum_i \delta x_i = 0. \tag{23}$$

These two constraints are included in the minimization via Lagrange multipliers λ and θ. A variation of the x_i in Eq. (17) gives

$$\delta F_{xs} = \sum_i \left(2\sum_j x_j F_{ij} + K_i \right) \delta x_i, \tag{24}$$

with

$$K_i = -\frac{1}{2(2\pi)^3} k_B T \int d\mathbf{q}[c_{ii}(q) - h_{ii}(q)]. \quad (25)$$

The c_{ii} are the diagonal direct correlation functions in the HNC approximation. Finally, the total variation of the free energy F is of the form

$$\delta F = \sum_i F^{\text{ion}} \delta x_i + F^{\text{elec}}(\delta \overline{n}/\overline{n}) = 0, \quad (26)$$

$$F^{\text{ion}} = k_B T(\ln x_i + 1) + \xi_i + \lambda Z_i - \theta,$$
$$F^{\text{elec}} = Z^*(\mu + \eta - \lambda),$$
$$\xi_i = F_i + L_i + 2\sum_j x_j F_{ij} + K_i,$$
$$\eta = \left(\sum_i x_i(f_i + l_i) + \sum_{ij} x_i x_j f_{ij}\right) \Big/ Z^*.$$

From Eq. (26) the ion concentrations x_i that minimize the total free energy are given by

$$x_i = A \exp[-\beta(\xi_i + \lambda Z_i)], \quad (27)$$

where A is chosen such that $\sum_i x_i = 1$ and

$$\lambda = \mu + \eta. \quad (28)$$

We note that λ is *the electron chemical potential inclusive of the effect of the ion-electron and ion-ion interactions.* Such corrections to the chemical potential contribute to effects loosely called "continuum lowering." The effect of the electron-electron interactions on the electron chemical potential [cf. Eq. (5)] is already contained in μ.

D. Calculation of other thermodynamic functions

When the concentrations x_i and other relevant quantities are determined, the calculation of the thermodynamic functions follows. As an example, we give the expression for the pressure P of the system. Thus differentiating the free energy with respect to volume

$$P\Omega = k_B T + \tilde{P}_e + \tilde{P}_{\text{em}} + \tilde{P}_{\text{ion-ion}}, \quad (29)$$
$$\tilde{P}_e = Z^* \overline{n} \frac{df(\overline{n})}{d\overline{n}} + Z^* \eta,$$
$$\tilde{P}_{\text{em}} = \sum_i x_i K_i,$$
$$\tilde{P}_{\text{ion-ion}} = \sum_{ij} x_i x_j F_{ij} + \frac{k_B T}{2\rho} \int \mathbf{F}(q;\rho) d\mathbf{q}.$$

Here $k_B T$ is the ideal gas ionic contribution, while $\tilde{P}_e$, proportional to Z^*, is the pressure contribution of the interacting uniform electron gas whose free energy per electron is $f(\overline{n})$ plus a term involving η, which is a correction to the electron gas pressure due to "continuum lowering effects." The term $\tilde{P}_{\text{em}}$ is a pure "embedding" contribution, while the two terms in $\tilde{P}_{\text{ion-ion}}$ arise from the embedded ion-ion interactions.

E. Calculation of the electrical resistivity

The simplest plasma resistivity calculations use the Spitzer formula, which is in many ways like Saha theory, in using many simplifying assumptions. Fully ionized hydrogen plasmas in the weak electron-ion coupling regime can be treated following Ichimaru and Tanaka's work [26]. Lee and More, Cauble and Rozmus, and Rinker [27] have presented resistivity calculations for more general plasmas. An objective of some of these models is the ease of on line calculation. Since we are interested in a microscopic approach we use the extension of the Ziman formula [28,29] to finite temperatures. We use the elastic scattering cross section $\sum(q)$ expressed in terms of the local pseudopotentials $w(q)$ and the HNC structure factors $S(q)$. The pseudopotentials $w(q)$ have already been encountered in Eq. (15). The resistivity is given by

$$R = -\frac{\hbar}{e^2}\frac{1}{3\pi}\frac{1}{Z^*\overline{n}} \int_0^\infty d\varepsilon \frac{df_{\text{FD}}(\varepsilon)}{d\varepsilon} \int_0^{q_m} q^3 \Sigma(q) dq, \quad (30)$$

with $f_{\text{FD}}(\varepsilon)$ the Fermi-Dirac occupation number for a level of energy ε. The upper limit q_m for the q integration is $(2/\hbar)\sqrt{2m\varepsilon}$. In the case of local pseudopotentials, this expression is readily transformed into

$$R = \frac{\hbar}{e^2}\frac{1}{3\pi}\frac{1}{Z^*\overline{n}} \times \int_0^\infty (1 + \exp\{\beta[\varepsilon(q)/4 - \mu]\})^{-1} q^3 \Sigma(q) dq, \quad (31)$$

with

$$\varepsilon(q) = \frac{(\hbar q)^2}{2m},$$
$$\Sigma(q) = \sum_{i,j} (x_i x_j)^{1/2} S_{ij} [w_i(q)/2\pi\mathcal{E}(q)][w_j(q)/2\pi\mathcal{E}(q)],$$
$$S_{ij} = \delta_{ij} + \rho(x_i x_j)^{1/2} h_{ij}(q).$$

The cross section $\Sigma(q)$ involves the electron gas dielectric function $\mathcal{E}(q)$ defined in Appendix A. The Ziman formulation treats only elastic scattering processes. The inelastic effects are small except at very high temperatures. The full T-matrix form discussed in our previous studies [29] is required only at sufficiently high temperatures. Some examples of the differences between a pseudopotential approach and a T-matrix approach will be given in Sec. III. The "Born-approximation-like" form used in Eq. (31) is valid because the pseudopotentials $w(q)$ have been constructed to be weak and is well established in the context of simple liquid metals. This form of the Ziman formula does not contain corrections arising from the modifications to the continuum density of states wherein the electron mass m gets replaced by a k-dependent effective mass $m^*(k)$ and other effects due to electron localization effects. While the thermodynamic properties are less sensitive to such effects, they can be important in quantitative predictions of transport coefficients. Thus the results obtained from Eq. (31) should be considered as a good first approximation that needs further corrections depending on specific experimental conditions. The following remarks should be noted.

(i) The Ziman formula corresponds to the simplest variational solution of a transport equation. Higher-order terms (arising from other basis functions) become impor-

tant in certain problems.

(ii) If the neutral-pseudoatom construction that involves the use of a cavity surrounding the scatterer ion (e.g., Al^{3+}), is *not* used, then the resistivity of the (Al^{3+}) fluid is found to grossly disagree with experiment (e.g., in molten aluminum fluid), while the NPA approach gives excellent agreement in the case of simple metallic systems such as Al^{3+}.

(iii) The resistivity calculated from the Ziman formula can be rewritten to define an "electron-ion" collision time $\tau_{e\text{-}i}$. Such a collision time defines a "transport" time that is different from the collision time that enters into energy relaxation.

The calculation of some of the other linear transport properties (e.g., thermal conductivity) follows in a simple manner and will not be considered here.

III. APPLICATION TO ALUMINUM PLASMAS

Aluminum plasmas provide both experimental and theoretical material for plasma studies. An aluminum target shocked by a laser pulse can generate a compressed hot plasma, which finally escapes in a plume consisting of an expanding plasma. The theoretical infrastructure needed for the interpretation of such experiments needs to be built up, within the equilibrium, Hugoniot, and nonequilibrium contexts. We also note that the phase diagram and the resistivity of expanded metal vapors near the critical point have attracted considerable attention [5] of experiments using more traditional techniques. Such metal vapors contain many neutral (and charged) clusters and fall somewhat outside the present study where we limit ourselves to single-center DFT calculations. That is, we consider only simple Al plasmas containing no stable ionic molecules (e.g., Al_2^{z+} or Al_2). In the expanded plasma regime we consider three temperatures, viz., 1.5 eV, 5 eV, and 10 eV. At 1.5 eV it was necessary to study the phase equilibrium among three phases, viz., A, containing Al^{z_i+}, $Z_i = 0, 1, 2, 3$, together with B, containing Al^{z_i+}, $Z_i = 1, 2, 3$, and C, containing only $Z_i = 3$. At 1.5 eV there is a region of coexistence between phases B and C that involves a phase transition in the plasma state reminiscent of metal-insulator transitions found in expanded metal vapors. At 5 eV and 10 eV there is no longer a coexistence region between phases B and C. The high density equilibrium regime, up to a compression of about 3, as well as the behavior along the standard shock Hugoniot can be treated quite well by DFT–average-atom models with $Z^* = 3$ and we present results for those regimes as well. This numerical work has been motivated by the need to test simplified ionization and conductivity models, which are more approximate but computationally simpler, and for the design and interpretation of laser-pulse experiments in these regimes.

A. Expanded plasma regime

Our calculations provide an opportunity to test the frequently used average-atom (AA) models, which do not contain the effects of ion-ion interactions and electronic configuration effects on the degree of ionization and related properties. Another shortcoming of AA models is that there exists a minimum density below which the numerical calculation becomes unstable for open shell atoms in jellium. The reason for the instability is the following. Let us consider Al at zero temperature and assume that, at a given iteration of the Kohn-Sham potential, the $3p$ level exists (as in the free atom). Then the average-atom–DFT scheme with a standard local density exchange-correlation functional requires us to fill this level with six electrons, leading to the configuration of an Al^{5+} ion. Thus the number of screening electrons in the displaced density of the scattering states must be 5. When the average free electron density is very low, this situation becomes highly unstable [30] and no self-consistent solution can be obtained. When the average structure description is abandoned and replaced with a treatment of distinct species, the number of electrons in the scattering states for the important configurations is much smaller, so that the numerical process is found to be stable. For the conditions of this study, at T =1.5 eV we need to treat the species Al^0, Al^{1+}, Al^{2+}, and Al^{3+}, but no stable clusters (e.g., Al_2) were needed, as discussed below. First we describe the determination of the density regime where the Al_2 molecule does not exist.

B. Existence of Al_n molecules ($n \geq 2$) in a plasma

The free Al_2 molecule has a binding energy of 1.55 eV and a bond length $R = 4.66$ a.u. ($^3\Sigma_g^-$ state) [31]. Detailed experimental information on molecular clusters Al_n, $n > 2$, does not exist. Several theoretical efforts for treating Al_n in vacuum have been reported [32,33] for n = 2–13. Bauschlicher *et al.* [32] found in their *ab initio* calculations using correlated wave functions that the maximum value of the binding energy per atom is 1.47 eV for $n = 6$, with a bond length $R = 5.24$ a.u., close to the interatomic distance in bulk metallic Al. More recently Jones [33] found that the binding energy per atom in Al_n clusters increases quasiregularly with n towards a value close to the cohesive energy of an atom in metallic Al at normal density. Although the binding energies for $n = 6$ calculated by these different authors do not agree, the results suggest that the nature of binding remains the same when going from small clusters to the metallic solid. Only the strength of this binding is affected.

In the free molecular Al_2, the binding energy curve is the negative of the pair potential. But when the number of atoms in the cluster increases, the cohesive energy consists of a contribution depending on the average electron density and a contribution arising from the pair potentials. In fact, stabilized jellium models [34] attempt to capture most of the stabilization via a suitable "electron gaslike" model. Thus metallic binding does not require a strongly attractive pair potential, unlike molecular binding. Returning to our present study, we assume that stable molecular clusters cannot exist in an electron gas at zero temperature if the pair potential is positive for a separation R equal to the bond length of the free molecule.

Let us consider the binding energy

$$D(R,\overline{n}) = \mathcal{E}(\infty,\overline{n}) - \mathcal{E}(R,\overline{n}). \quad (32)$$

Here $\mathcal{E}(R,\overline{n})$ denotes the energy of the molecule in the electron gas at electron density $\overline{n}$, when the interatomic distance is R. In Appendix C we describe an approximate method for estimating the change δD in D due to embedding Al_2 in an electron gas with density $\overline{n}$:

$$\delta D(R,\overline{n}) = D(R,\overline{n}) - D(R,0). \quad (33)$$

We use a model that, when applied to the embedding of the H_2 molecule, is found to give good agreement [35] with more fundamental calculations. Taking [32] $D(R,0)$ = 3 eV approximately, we determine the "critical" density $n_{\rm crit}$ for which δD reaches the value -3 eV. As discussed in Appendix C, we have calculated δD at the equilibrium distance of the free molecule for various electron densities and found that this quantity reaches -3 eV around $\overline{n}$ = 0.0008 a.u., that is, for a density 32 times smaller than the normal metallic electron density n_0 of Al (i.e., r_s =2.07 a.u.). We conclude that, at zero temperature, one can expect that two Al atoms will not form a stable molecule if the electron density is larger than a critical density $n_{\rm crit}$, which is of about $n_0/32$. For higher temperatures, the binding energy is certainly smaller so that the formation of a stable molecule is even less probable.

C. Results

1. T = 1.5 eV

We have done calculations in aluminum for illustrating the model described in Sec. II. The lowest temperature considered is T = 1.5 eV, well above the critical temperature, which is estimated [36] to be T_c = 0.68 eV. The reported [36] critical matter density is 0.73 and corresponds to a compression ρ_c/ρ = 0.27. In Tables I–III we show the results, namely, embedding free energies, embedding internal energies, and eigenvalues for the outermost electrons, obtained for the dominant configurations. We see that the $3p$ level does not exist for electron densities higher than $n_0/16$, so that neutral species disappear above this density. As in DFT calculations for average atoms using a single structure with average ionic charge Z^* (average-structure model), there are ranges of densities where a bound level delocalizes and extends outside the average volume that can be attributed to each atom. In the range of densities where the delocalization occurs, the simple metal picture loses its meaning, due to the existence of shallow states that, although they do not form stable clusters, are weakly bound to several ions. Such states are expected to form when sharp features exist in the density of states of the "continuous" spectrum. In these density ranges, pair potentials cannot be constructed and we are not able to predict the structure of the fluid within the scheme used in this work. This is the case for $n_0/32 < \overline{n} < n_0/16$ (delocalization of the $3p$ level) and for $n_0/4 < \overline{n} < n_0/1.5$ (delocalization of the $3s$ level). This appears in Fig. 1, where the total free energy of the fluid is plotted versus compression. The corresponding numbers are reported in Table III. In Fig. 1, we see three solid curves A, B, and C. Curve A corresponds to hypothetical states of the fluid made of a mixture of atomic (i.e., neutral Al) and ionic species only, with no molecules. These states are hypothetical because the discussion of Sec. III B shows that molec-

TABLE I. Embedding free energy F_i, internal energy E_i, and eigenvalues $\epsilon_{3s}, \epsilon_{3p}$, for the charge states Z_i that exist at selected electron densities $\overline{n}$ in an Al plasma at T = 1.5 eV. Energies are in rydbergs. The density $\overline{n}$ is given as a fraction of the normal density n_0 = 0.027 a.u. (r_s = 2.07 a.u.) of electrons in solid Al. Levels with negligible occupation are marked with an asterisk while the ellipsis indicates the absence of the charge state.

T = 1.5 eV	$Z_i=0$	$Z_i=1$	$Z_i=2$	$Z_i=3$
		$\overline{n}=(n_0/64)$		
$-F_i$	482.7926	482.3950	...	...
$-E_i$	482.6066	482.3877	...	...
$-\epsilon_{3s}$	0.4167	0.5540	...	...
$-\epsilon_{3p}$	0.0576	0.1517	...	...
		$\overline{n}=(n_0/32)$		
$-F_i$	482.7114	482.3850	481.6377	...
$-E_i$	482.5018	482.3653	481.5043	...
$-\epsilon_{3s}$	0.3822	0.4649	0.6967	...
$-\epsilon_{3p}$	0.0329	0.0760*	0.2559*	...
		$\overline{n}=(n_0/16)$		
$-F_i$	...	482.7017	482.2269	...
$-E_i$	...	482.6808	482.1585	...
$-\epsilon_{3s}$	...	0.1750	0.2560	...
		$\overline{n}=(n_0/8)$		
$-F_i$	...	482.7659	482.3029	481.6261
$-E_i$	...	482.7212	482.1879	481.6255
$-\epsilon_{3s}$	...	0.1033	0.1565	0.2268
		$\overline{n}=(n_0/1.5)$		
$-F_i$	...	...	...	482.8144
$-E_i$	...	...	...	482.7998
		$\overline{n}=n_0$		
$-F_i$	...	...	...	483.0078
$-E_i$	...	...	...	482.9917

TABLE II. Compression ρ/ρ_0, average ionization Z^*, and composition x_0, x_1, x_2, x_3 calculated in the present theory, for Al at T = 1.5 eV. If x_i is given as 0.0000, then $x_i < 0.5\times10^{-4}$. The ellipsis implies the absence of the charge state Z_i.

$\overline{n}/n_0$	ρ/ρ_0	Z^*	x_0	x_1	x_2	x_3
1/64	0.348	0.135	0.865	0.130	0.000	0.000
1/32	0.844	0.111	0.889	0.111	0.000	0.000
1/16	0.159	1.176	...	0.824	0.176	0.000
1/8	0.312	1.202	...	0.804	0.188	0.007
1/4	0.507	1.479	...	0.614	0.294	0.092
1/1.5	0.667	3.000	...	...	...	1.000
1	1.000	3.000	...	...	...	1.000

TABLE III. Compression ρ/ρ_0, total Helmholtz energy F, Gibbs energy G, internal energy E, total pressure P ($\times$ atomic volume Ω), and electrical resistivity R, for Al plasma at $T = 1.5$ eV. The energies are in Ry/atom, while R is in $\mu\Omega$ cm.

$\overline{n}/n_0$	ρ/ρ_0	$-F-480$	$-G-480$	$-E-480$	$P\Omega$	R
1/64	0.348	4.435	4.059	2.325	0.376	887
1/32	0.844	3.770	2.611	1.823	1.159	1000
1/16	0.159	4.818	4.648	2.449	0.170	2173
1/8	0.312	4.688	4.438	2.447	0.250	802
1/4	0.507	4.469	3.990	2.283	0.479	335
1/1.5	0.667	4.638	4.225	2.635	0.383	71.5
1	1.000	4.490	3.882	2.609	0.608	35.3

ular states are likely to exist for the electron densities involved ($\overline{n} < n_{\rm crit} < n_0/32$). Curve B corresponds to electron densities $n_0/16 < \overline{n} < n_0/4$, where the fluid is a mixture of $Z_i = 1$, 2, and 3 ionic species, but with no neutral Al atoms. Molecular species are improbable at these electron densities so that the fluid states discussed here may really exist. The calculations show that they are more stable (by 2.5 eV) than the hypothetical states with neutral atoms. They cover a range of compressions between 0.1 and 0.5, including the critical compression (0.27). The stabilization free energy gained in increasing the free electron charge density is larger than the energy required to bind the $3p$ electron. Here it would be useful to know where the curve for a fluid containing neutral Al_n molecules would be. Because we cannot make a reliable calculation for a fluid containing molecules, we can only give the following imprecise argument. In the most stable molecular state, the binding would be increased by approximately 1.5 eV per atom involved. Thus a fluid having a concentration x_0 of neutral atoms in molecular form would have a free energy lower by $0.1x_0$ Ry/atom

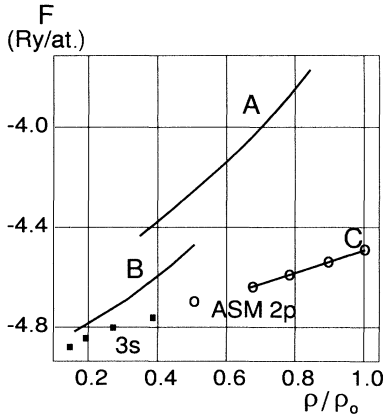

FIG. 1. Total Helmholtz free energy per atom of Al at $T = 1.5$ eV as a function of the compression ρ/ρ_0. Curve A is for the unstable fluid with Z_i =0, 1, and 2, in the free electron density range $1/64 < \overline{n}/n_0 < 1/32$; curve B is for the fluid with Z_i =1, 2, and 3, with $1/16 < \overline{n}/n_0 < 1/4$; curve C is for the fluid with $Z_i = 3$, with $1/1.5 < \overline{n}/n_0 < 1$. The average-atom model [see Eq. (34)] results are shown as solid squares (the ASM $3s$) and as open circles (the ASM $2p$). Note that ASM $2p$ merges with MSM in curve C.

than the fluid described by curve A for a fixed ionization. Obviously, such a conclusion holds only if all the other contributions to energy are roughly the same. This lowering would be approximately of 0.1 Ry/atom for any state shown in curve A. This is not enough to stabilize these states with respect to those of curve B. Thus curve B probably represents the actual fluid state in the range of compressions 0.1–0.5, at a temperature of 1.5 eV. Finally, curve C corresponds to a fluid where only the $Z_i = 3$ configuration exists. In this part of the curve, the average ionization Z^* is also 3 and the multispecies model (MSM) and the average-structure model (ASM) become equivalent. The fluid states in C are similar to those of liquid Al under normal conditions. For the reasons mentioned above, the model is not able to describe the transition from curve B to curve C.

The ASM results are also shown in Fig. 1 as open circles, joined where relevant by a dotted line. It appears that the ASM free energies are lower than those of the MSM. Although the Mermin-Kohn-Sham equations for the average atom in the electron gas should, in principle (i.e., if they were solved exactly with the exact exchange-correlation energy functional and in the same external potential), give the same electronic free energy as the multiconfigurations equations, there is no reason to believe that this is the case in practice. The main reasons for the differences are (i) the inclusion of an effective degeneracy D_{nl}, as discussed below, in the ASM where bound electrons are confined to a single atomic volume Ω of the average ion; (ii) the correction of the electronic entropy in the MSM as discussed in Eq. (8); (iii) the use of a LDA–exchange-correlation-functional that favors double occupancy of bound states as T goes to 0 K; (iv) the ASM and MSM differ in the treatment of the ion-ion interactions, which depend on Z_i in the MSM and Z^* in the ASM; and (v) the difference in the estimates of Z^* in the two models implies that, for the same $\overline{n}$, we are in fact looking at two different matter densities ρ in the two models.

We comment further on some of these issues. In the ASM, the DFT calculation deals with a single "average" ion whose structure may be specified by its highest bound state (e.g., the ASM $2p$ has no $n = 3$ shell). The electronic levels are populated according to Fermi-Dirac statistics. An effective degeneracy D_{nl} is attributed to each bound level n, l in order to exclude from the bound charge the part that extends outside the average atomic sphere of volume Ω. This degeneracy is

$$D_{nl} = 2(2l+1)\int_{\Omega} |\phi_n l(r)|^2 d\mathbf{r}, \tag{34}$$

where $\phi_n l(r)$ is the wave function of the n, l bound state, having an energy ϵ_{nl}. The average ionization is then $Z^* = Z - \Sigma_{nl} D_{nl} f_{\rm FD}(\epsilon_{nl})$. Then a single average pair potential is built using the same technique as described in the MSM case and the HNC equation is solved for the *single* species fluid. As shown in Fig. 1, the total free energy resulting from this model turns out to be lower than that of the MSM. The ionization Z^* of the ASM is controlled only by the electronic distribution of a single

average ion in an average cavity, while the Z^* of the MSM is *constrained* to depend on both the electronic and ionic distributions. For instance, for $\overline{n} = n_0/4$, one finds $Z^* = 1.953$ (ASM) and 1.479 (MSM); for $\overline{n} = n_0/8$, $Z^* = 1.406$ (ASM) and 1.202 (MSM). A direct consequence is that, for the same electron density, the resulting matter densities are different in the two models.

In Fig. 2 we have plotted the total Gibbs energy $G = F + P\Omega$ versus pressure, also shown in Table III, for the three regimes of ionization. Consider the equilibrium between these "possible" phases. The crossover of the curves relative to "phases" B and C would determine the values of the thermodynamic variables at the transition. Because the model cannot produce the entirety of the curves, curve C of Fig. 2 needs to be extrapolated as indicated. The intersection with curve B occurs for a pressure $P\Omega_0 = 0.06$ Ry (80 kbar) and compressions between 0.27 and 0.40. It is remarkable that the lowest compression corresponds closely to the critical density. The variations of pressure ($\times\Omega_0$) with density are shown in Fig. 3. The average number of free electrons per atom is expected to increase rapidly from 1.2 to 3 in this interval, suggesting some form of a plasma phase transition [4]. If the ASM were used, the pressure versus compression curve is smooth, as shown by the dotted curve passing through the open circles. Here again we note that the average-structure DFT becomes equivalent to curve C for compressions greater than 0.66. The pressure versus compression predicted by the Sesame Library (tables of data published by the Los Alamos Scientific Laboratory) is shown by squares in Fig. 3.

Coherently with the previous discussion of curve A, which was calculated without allowing for molecular structures such as Al_n, we see in Fig. 2 that B and A will never cross. The most probable situation is that B will intersect an unknown curve describing the Gibbs energy of a complex fluid containing ions, atoms, and molecules, for a compression lower to 0.27.

Figure 4 shows the average ionization Z^* as a function of the compression for the MSM and ASM. These

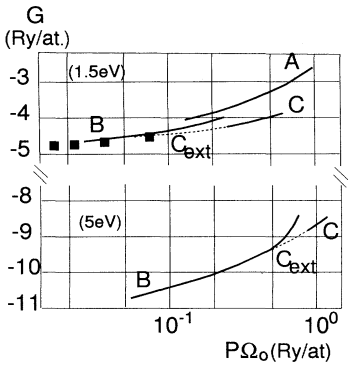

FIG. 2. Total Gibbs free energy per atom of Al at $T = 1.5$ eV as a function of $P\Omega_0$, i.e., (pressure) $\times$ (normal atomic volume) of Al. Curves A–C and the ASM $3s$ results at T=1.5 eV are shown in the top part. C_{ext} is the extrapolation of curve C to cover the discontinuity due to the ionization of the $3s$ level. Results for $T = 5$ eV are given in the lower half. Here the unstable phase (analog of curve A) does not exist.

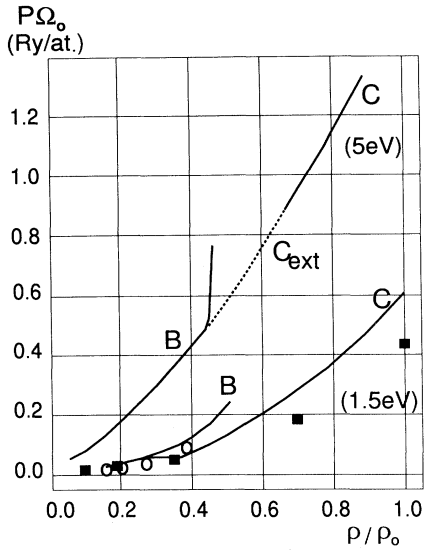

FIG. 3. $P\Omega_0$ as a function of compression. Curves B and C are as in Figs. 1 and 2. The open circles are ASM $3s$ data points, while the solid squares are from the *Sesame* tables, for $T = 1.5$ eV.

Z^* values enter into the electrical conductivity (Fig. 5) calculated in the three regimes. The resistivity for the unstable regime A is remarkably constant. The values in curve B are valid for $\rho/\rho_0 < 0.27$ and those of curve C are reliable everywhere. An interpolation between the two later portions of curve is possible and gives a reasonable estimate of R. The ASM resistivity is also shown. In the lowest range of compressions, it is lower than the MSM resistivity. In Table IV we compare the difference

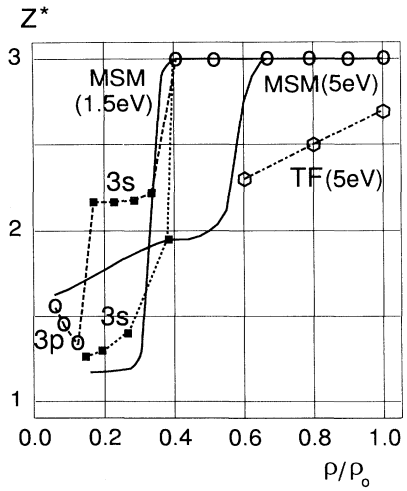

FIG. 4. Average ionization Z^* as a function of compression for $T = 1.5$ and 5 eV. Points in discontinuous ASM branches are joined by dashed lines merely to guide the eye (the long-dashed line is 5 eV and the short-dashed line is 1.5 eV). Solid curves are from the MSM approach. Three data points (open hexagons) are from a Thomas-Fermi model [37] at 5 eV.

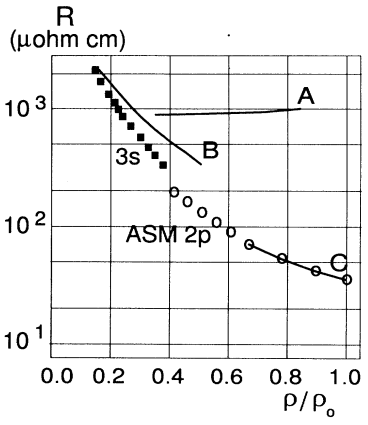

FIG. 5. Electrical resistivity of expanded Al at $T = 1.5$ eV. The curves and data points are as in Fig. 1.

between the pseudopotential and T-matrix results of the resistivity, using the ASM approach. The MSM pseudopotential resistivity was given in Table III.

2. $T = 5$ and 10 eV

Here we explore the same density range (compression $\kappa = \rho/\rho_0$) as before, but at higher temperatures. The main difference between the low temperature ($T = 1.5$ eV) case is that the phase A, containing neutral Al, is totally out of the picture and there is no longer any extended coexistence region between phases B (a mixture of Al^{z_i+}, Z_i =1, 2, and 3) and phase C (which has only $Z_i = 3$). However, it turns out that at $T = 5$ eV there is a coexistence *point* in that the pressure versus density curves overlap at $P\Omega_0 = 0.45$ Ry/atom. In Fig. 2, lower part, we show how the Gibbs free energy calculated for phases B and C varies with pressure, calculated using the MSM. There is a region where the calculation cannot be done due to the disappearance of $3p$ and $3s$ levels. However, extrapolation of curve C as shown in the figure can be carried out. Thus, in Fig. 3 we see how the plasma phase transition at $T = 1.5$ eV transforms itself to the single coexistence point at $T = 5$ eV and about $\kappa \sim 0.45$.

TABLE IV. The average ionization Z^* calculated using an appropriate model is tabulated as a function of temperature and electron compression $\overline{n}/n_0$. Thus the material compression ρ/ρ_0 is $(3/Z^*)(\overline{n}/n_0)$. The row labeled 10^2TF gives Z^* at 100 eV calculated using a simple Thomas-Fermi [37] model.

$\overline{n}/n_0$	1/32	1/16	1/8	1/4	1/2	1	2
T (eV)							
1.5	1.160	1.176	1.202	1.479	3.000	3.000	3.000
5.0	1.625	1.675	1.718	1.948	3.000	3.000	3.000
10	2.260	2.310	2.362	2.455	3.027	3.023	3.018
40	6.241	5.883	5.574	5.204	5.107	5.193	5.140
100	10.29	9.966	9.585	9.198	8.665	8.272	7.978
10^2TF	9.22	8.21	8.40	7.96	7.52	7.11	6.78
400	12.88	12.79	12.67	12.48	12.16	11.88	11.57
1000	13.00	12.98	12.97	12.96	12.94	12.92	12.84

In Fig. 6 we compare the variation of $P\Omega$ as a function of the compression κ, with $T = 5$ and 10 eV, together with the predictions from the average atom (i.e., the ASM) calculations. Here the ASM used is identified by the last bound state that exists in the average structure: ASM $3p$, ASM $3s$, and ASM $2p$. The ASM $2p$ corresponds to $Z^* = 3$ and hence merges with phase C calculated using the MSM.

It is interesting to see how these differences (between the different theoretical models) appear in the predicted ionization Z^*. In the Saha model (as implemented by Kerley [10]), with T=1.5, 5, and 10 eV, at a free electron density $\overline{n} = n_0/32$, where n_0 is the electron density in solid Al at room temperature, Z^* is predicted to be 0.345, 0.469, and 1.44, respectively. The MSM gives Z^*= 1.160, 1.625, and 2.260, respectively, showing the well known limitations of the Saha model. In Fig. 4 we compare Z^* for the ASM and MSM at T=5 eV. The Z^* from ASM contains several discontinuous segments. Thus ASM $3p$ ionization *decreases* with increasing compression, jumps abruptly to the ASM $3s$ curve where R is rather flat, and then joins the MSM curve to give an Z^*=3. For the higher compressions, we also show (open hexagons) the Z^* obtained from a popular Thomas-Fermi model [37]. These differences in the predicted Z^* and the state properties of the fluid reveal themselves in the transport properties as well. Thus, in Fig. 7 we show the electrical resistivity as a function of compression for $T = 5$ eV (lower panel) and $T = 10$ eV (upper panel). The large (unphysical) discontinuities in the ASM values of R correspond to those of Z^* shown in Fig. 4. In Table IV we compare the pseudopotential and T-matrix evaluations of R, within the ASM model, at $T = 5$ and 10 eV. Clearly, prediction of plasma transport properties with confidence requires detailed attention to the atomic physics of the plasma.

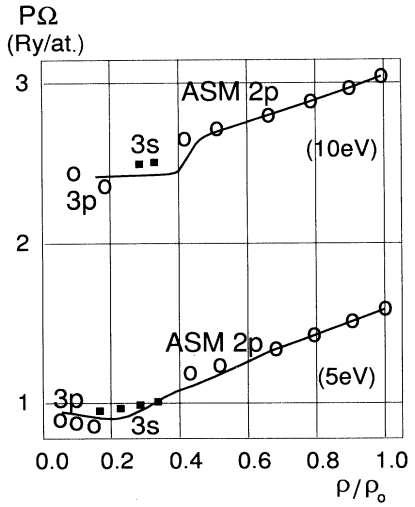

FIG. 6. $P\Omega$ as a function of compression at $T = 5$ and 10 eV. Here Ω is the average volume per atom. The average-atom results (ASM) for $3p$, $3s$, and $2p$ are given as data points for comparison with the full curves obtained from the MSM approach.

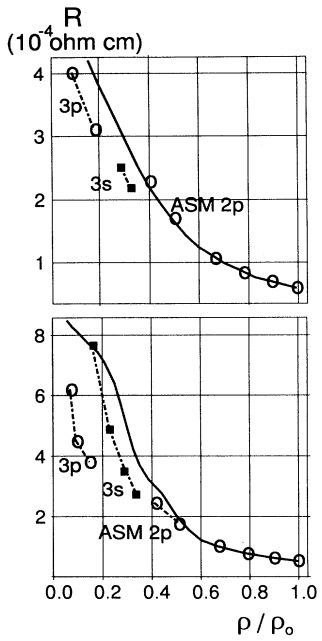

FIG. 7. Electrical resistivity of Al as a function of compression using pseudopotentials. Upper panel, $T = 10$ eV; lower panel, $T = 5$eV. The average-atom model resistivities are indicated by data points labeled ASM $2p$ and ASM $3p$. The dotted line through the ASM points is a guide to the eye. The solid line is the MSM resistivity.

3. *Compressed and shocked plasmas*

The higher compression regime ($\kappa > 1$) is relatively simple up to about $\kappa = 3$ since the ionization state of the Al plasma is essentially Z^*=3. Thus the MSM and the ASM merge into each other. For $\kappa > 3$ we again get into regions where the average number of free electrons per ion becomes fractional due to the formation of bands and pressure ionization at low temperatures. The previous analysis cannot be applied without modification, although the idea of using several neutral pseudoatoms to formulate the theory might still be relevant. However, most shock experiments and laser pulse experiments remain in the regime of $\kappa < 3$ and hence we do not discuss these extreme high pressure regimes here. Tables IV and V provide a "bird's-eye view" of the variation of the average ionization and resistivity of expanded and compressed Al plasmas as a function of temperature and density. In practice, high compression experiments that satisfy the conditions of the shock Hugoniot are of great interest since the compression and the temperature of the plasma can be connected via the EOS. At high compressions and high temperatures the details of the ion-ion structure factor become unimportant as far as the transport properties are concerned. But now the full T matrix discussed in our previous studies [29] becomes necessary. Suitable calculations for the standard shock Hugoniot are given in Table VI.

TABLE V. Electrical resistivities R ($\mu\Omega$ cm), calculated using the ASA model and showing (where necessary) the results from the pseudopotential (labeled w) and the T-matrix (labeled t) versions of the scattering cross section (see the text). The MSM-pseudopotential resistivities were given in Table III. Nonconvergence of the calculations is indicated by NC. Note that at $T = 5$ eV, for $1/16 < \overline{n}/n_0 < 1/4$, the w resistivity is discontinuous due to the ionization of the $3p$ state, while the t resistivity is continuous.

$\overline{n}/n_0$	1/32	1/16	1/8	1/4	1/2	1	2
T (eV)							
1.5w	NC	2133	708	315	127	35.3	17.0
1.5t	2310	1662	863	423	155	41.2	35.8
5.0w	608	371	767	273	165	52.1	18.1
5.0t	946	772	593	401	243	70.8	47.9
10.0w	NC	395	304	252	168	59.0	20.4
10.0t	633	534	452	357	279	108	76.1
40.0t	420	252	280	238	187	153	120
100t	262	189	150	132	114	97.5	81.0
400t	70.6	64.5	58.2	51.9	45.4	39.2	33.3
1000t	21.9	20.4	18.9	17.4	16.0	14.5	13.0

IV. CONCLUSION

We have described a first-principles method of calculating the thermodynamics (e.g., ionization balance and equation of state) and transport properties of plasmas for a very wide range of densities and temperatures. The regimes include expanded plasmas at low temperature and densities where atomic and ionic species can exist, as well as shock compressed and other plasmas. We have used an analytical approach rather than a molecular dynamics (MD) approach, although the ideas can be easily adapted to a simulations approach. That is, once the embedding energies and pair interactions were given, MD methods can be used for the calculation of thermodynamics and other properties. The present theory reduces to the conventional Saha model under the following approximations: ion-ion interactions are neglected, the total energy of any ionic species is replaced with its limit at infinite dilution, and electron density effects are described by some form of continuum lowering. The main features of the present approach are (i) instead of using semi-empirical, quasichemical, hard-sphere-type descriptions of density effects, all the electronic energies required are self-consistently calculated using DFT concepts; (ii) the ion-ion interactions, calculated from outputs of the previous step, are explicitly used in the total free energy, which is minimized to get the concen-

TABLE VI. Electrical resistivity R ($\mu\Omega$ cm) along the shock Hugoniot of aluminum $Z^* \simeq 3$ with the initial conditions for the shock exactly at the normal solid Al density at 300K. The compression is ρ/ρ_0.

T (eV)	0.25	0.50	1.00	2.50	5.00	10.0	15.0
ρ/ρ_0	1.57	1.70	1.89	2.26	2.59	2.97	3.22
R	31.57	32.65	33.75	36.08	43.67	61.57	74.38

trations of the various species; and (iii) ion-ion correlations are treated via the structure factors obtained from the HNC integral equations. Possible molecules or clusters are not introduced in the present description. This could be done without formal difficulties, but the numerical determination of the interaction energy of molecules or clusters in the plasma is a complex problem within a first-principles approach. The present model requires that different charge states can be identified. This is not possible when there are bound states (or quasilocalized continuum states) that are not contained inside the Wigner-Seitz sphere around each nucleus. In these regimes there are not just bound electrons and free electrons, but also "hopping electrons" that experience the potential of two or more nuclear centers and single-center models and simple metal models may not be adequate. Regimes corresponding to the delocalization of the $3s$ and $3p$ levels were explicitly pointed out in this study. At higher compressions and temperatures, not discussed in this work, there would be other regimes corresponding to the delocalization of $2p$ and $2s$ levels where the present type of theory needs further modifications.

The most important approximation made in this work is the use of a single-center neutral pseudoatom model with spherical boundary conditions and the restriction to integer ionization states. In order to assess the limitations of such an approximation it is necessary to compare the results with those from a many-electron finite temperature calculation for many atoms dynamically optimized from some set of random configurations. Such a calculation is feasible for a limited number of atoms using, e.g., the Car-Parinello method. A particularly stringent case would be molten Si, where many authors believe that bond directionality and covalent bonding persist locally in the liquid state. Such a comparison of our method, with a Car-Parinello calculation by Štitch *et al.* [38], using 64 atoms of Si in the simulation supercell was given in our study in [23(a)]. Those results show that the calculations based on the neutral Si-pseudoatom method are probably as good as or better than the supercell multicenter calculation where the latter yielded a statistically very noisy ion-ion structure factor $S(k)$. Liquid carbon was also studied and compared with the 54-atom multicenter Car-Parinello-type simulation by Galli *et al.* [38]. In effect, even in these extreme cases of group-IV elements at their melting points, the methods presented in this paper seem to be very useful in providing reliable results. This makes us confident that the plasma phase transition found in our calculations is well beyond any error limits of the single-center NPA approximation used here and represents the genuine physics of a mixture of atomic ions (i.e., no molecular states are involved).

Thus in the numerical example presented for Al at $T = 1.5$ eV, we have identified a domain of densities ($0.35 < \rho/\rho_0 < 0.9$ approximately) where an unstable state exists; this state results from a mixture of neutral atoms and ions with charges 1 and 2. It has a weak average ionization and a practically constant resistivity. Two stable regimes correspond to ions with charges 1, 2, 3 for $0.15 < \rho/\rho_0 < 0.5$ and charge 3 only for $0.5 < \rho/\rho_0 < 1$. A reasonable picture of the evolution of the state of the plasma as a function of the density can be obtained by assuming a transition between these two regimes in the range of compressions 0.27–0.40 at a pressure of 80 kbar. The rapid increase of ionization between the low ionization phase with $Z^* = 1.2$ to the high ionization phase with $Z^* = 3$, together with a rapid decrease of the resistivity, may suggest a plasma phase transition in the $T = 1.5$ eV Al plasma studied here. A sampling of results for a wide range of plasma conditions was given, the central theme of the paper being that calculations of transport properties of plasmas with confidence require detailed attention to the atomic physics of the plasma.

ACKNOWLEDGMENT

The authors are grateful to Annette Lecourt-Grimaldi for technical help in various aspects of this work.

APPENDIX A: DENSITY DERIVATIVE OF L_i

In this appendix we give an explicit form for l_i, the density derivative of L_i, defined in Eq. (11)

$$L_i = L_i^{(1)} + L_i^{(2)},$$
$$L_i^{(1)} = \eta_i(r) \otimes V_i(r),$$
$$L_i^{(2)} = -\frac{1}{2}\eta_i(r) \otimes \frac{1}{|\mathbf{r}-\mathbf{r}'|} \otimes [\nu_i(r') - m_i(r')],$$

where $\eta_i(r) = \overline{n} - \nu_i(r)$ and $l_i = \overline{n}\delta L_i/\delta\overline{n}$.

1. Density derivative of the first term $L_i^{(1)}$

The charge deficit $\eta_i(r)$ associated with the cavity of radius R_i is zero for $r < R_i$ and becomes $\overline{n}$ for $r > R_i$. Thus, when $\overline{n}$ changes by $\delta\overline{n}$, R_i changes by δR_i and $\eta_i(r)$ changes in magnitude and extension. Thus the density derivative of $L_i^{(1)}$ is

$$-\overline{n}V_i(R_i)\delta\Omega_i + \eta_i(r) \otimes V_i(r)(\overline{n}/\delta\overline{n}) + \eta_i(r) \otimes \delta V_i(r).$$

Using Eq. (13), this becomes

$$-f_i(\delta\overline{n}/\overline{n}) + \eta_i(r) \otimes \delta V_i(R_i). \tag{A1}$$

The variation $\delta V_i(R_i)$ can be calculated as follows, starting with

$$V_i(r) = -Z_i/r + [\nu_i(r') + \Delta n_i(r)] \otimes |\mathbf{r}-\mathbf{r}'|^{-1},$$

where $\Delta n_i(r)$ contains a bound-electron density $n_{bi}(r)$ and a free electron density displacement $\Delta n_{fi}(r)$. The bound density can be assumed not to change under the variation $\delta\overline{n}$. On the other hand, the change $\delta\Delta n_{fi}(r)$ can be related to the pseudopotential w_i of the ion. Thus we have, in Fourier space,

$$\delta V_i(q) = v(q)\delta\{\Pi(q,\overline{n})[w_i(q) + v(q)\nu_i(q)]\},$$

where $v(q) = 4\pi/q^2$ is the Coulomb potential and $\Pi(q,\overline{n})$

is the interacting electron-gas response function

$$\Pi(q,\overline{n}) = \Pi_0(q,\overline{n})/\mathcal{E}(q,\overline{n}),$$
$$\mathcal{E}(q,\overline{n}) = 1 - \{v(q) + X(0)\}\Pi_0(q,\overline{n}).$$

Here $\Pi_0(q,\overline{n})$ is the Lindhard function at density $\overline{n}$ and at the temperature T of the electrons. The finite temperature local field correction $X(q)$ is a constant in the $q = 0$ limit, consistent with the local density approximation to the exchange and correlation used in the DFT calculations [21]. Then, defining

$$K(q) = [\overline{n}/\Pi_0(q,\overline{n})][\delta\Pi_0(q,\overline{n})/\delta\overline{n}],$$

we can rewrite $\delta V_i(q)$ as

$$\delta V_i(q) = v(q)\{K(q)\Delta n_{fi}(q)(\delta\overline{n}/\overline{n}) + \Pi(q,\overline{n})v(q)\delta\nu_i(q)\}.$$

It can be verified that

$$\lim_{q\to 0} v(q)K(q) = -\overline{n}\frac{\partial}{\partial\overline{n}}[X(0) - 1/\Pi_{00}],$$

where Π_{00} is $\Pi_0(q=0,\overline{n})$. For a neutral pseudoatom the charge density $\Delta n_{fi}(r)$ integrates to zero, $v(q)\Pi(q,\overline{n})$ is finite at $q = 0$, and $\delta\nu_i(q)$ behaves like q^2. Then

$$\overline{n} \otimes \delta V_i(r) = -(Z_i^2/5R_i)(\delta\overline{n}/\overline{n}).$$

Hence, introducing the notation

$$U(q) = -v(q)m(q),\ m(q) = -\Pi(q,\overline{n})v(q)\nu_i(q),$$
$$\tilde{U}(q) = v(q)K(q)\Delta n_{fi}(q) + U(q),$$

we can evaluate $\eta_i(r) \otimes \delta V_i(R_i)$ needed in Eq. (A1) as

$$\eta_i(r) \otimes \delta V_i(R_i) = \frac{\delta\overline{n}}{\overline{n}}\left[Z_iU(R_i) - \frac{Z_i^2}{5R_i} - \int\frac{d\mathbf{q}}{8\pi^3}\tilde{U}(q)\nu_i(q)\right].$$

2. Density derivative of $L_i^{(2)}$

The expression for $L_i^{(2)}$ written in q space can be used to write its density derivative in the form $T_1(q) + T_2(q)$,

$$T_1 = -\delta\left\{\overline{n}\lim_{q\to 0} v(q)\nu_i(q)[1 + v(q)\Pi(q,\overline{n})]\right\}\Big/2,$$

$$T_2 = \frac{1}{2}\int\frac{d\mathbf{q}}{8\pi^3}\delta\{\nu_i(q)v(q)\nu_i(q)[1 + v(q)\Pi(q,\overline{n})]\}.$$

These can be rewritten as

$$T_1 = -\delta[Z_i\overline{n}\{X(0) - 1/\Pi_{00}\}]/2 + I_1,$$
$$I_1 = \int\frac{d\mathbf{q}}{8\pi^3}\delta\nu_i(q)[v(q)\nu_i(q) + U(q)],$$
$$T_2 = \frac{1}{2}\int\frac{d\mathbf{q}}{8\pi^3}\nu_i(q)v(q)\nu_i(q)v(q)K(q)\Pi(q,\overline{n})\frac{\delta\overline{n}}{\overline{n}}.$$

Further manipulation gives, for the first term in T_1,

$$-(1/2)Z_i\overline{n}[X(0)(1 + \Upsilon_{X(0)}) - (1 + \Upsilon_{\Pi_{00}})/\Pi_{00}](\delta\overline{n}/\overline{n}),$$

where we have defined

$$\Upsilon_{\Pi_{00}} = \overline{n}\Pi_{00}\frac{\partial(\Pi_{00}^{-1})}{\partial\overline{n}},$$
$$\Upsilon_{Xx(0)} = \overline{n}X(0)^{-1}\frac{\partial X(0)}{\partial\overline{n}}.$$

The integral I_1 can be transformed by considering successively the two contributions to the change in the magnitude and extension of the cavity ν_i. The change in magnitude gives

$$\int\frac{d\mathbf{q}}{8\pi^3}\nu_i(q)[v(q)\nu_i(q) + U(q)]\frac{\delta\overline{n}}{\overline{n}}$$

and can be regrouped with the term in $\delta\overline{n}/\overline{n}$ in T_2. The change in extension of ν_i manifests as a change δR_i in the cavity radius and gives the contribution

$$-[Z_i^2/R_i + Z_iU(R_i)]\,(\delta\overline{n}/\overline{n}).$$

3. Complete expression for the derivative of L_i

Putting together the results of the two previous subsections, we obtain

$$l_i = l_i^a + l_i^b,$$
$$l_i^a = -f_i + (1/2)Z_i\overline{n}[X(0)(1 + \Upsilon_{X(0)}) - (1 + \Upsilon_{\Pi_{00}})/\Pi_{00}],$$
$$l_i^b = \int\frac{d\mathbf{q}}{8\pi^3}\left[\Delta n_{fi}(q) - \frac{1}{2}\Pi(q,\overline{n})\nu_i(q)v(q)\right]\nu_i(q)v(q)K(q).$$

In obtaining this result, use has been made of the cancellation of $-6Z_i^2/5R_i$ with $(2\pi)^{-3}\int d\mathbf{q}\nu_i(q)v(q)\nu_i(q)$.

APPENDIX B: CORE-CORE REPULSIVE POTENTIALS

Consider two ions a and b located at positions R_i and R_j, in an electron gas of density $\overline{n}$. The interionic distance $|\mathbf{R_i} - \mathbf{R_j}|$ is R. The interaction between these ions involves Coulomb forces between the two nuclei, between the bound (i.e., core) electron, and between displaced free electron distributions, as well as cross terms and exchange-correlation effects. However, the most difficult issue is to deal correctly with the changes in the kinetic energy contributions to the interaction. In the following we treat this problem using Kohn-Sham concepts.

1. Notations

We use the following notation in this appendix. $n_{ai} = n_a(|\mathbf{r} - \mathbf{R_i}|)$ is the *displaced* electron density around the ion a. Also, n_a means $n_a(r)$. The free energy func-

tional containing the kinetic and exchange-correlation-contributions is denoted by $G[n+\overline{n}]$. We define

$$\Delta G[n+\overline{n}] = G[n+\overline{n}] - G[\overline{n}],$$

$$f_{ai} \otimes g_{bj} = \int d\mathbf{r} f_a(|\mathbf{r}-\mathbf{R_i}|) g_b(|\mathbf{r}-\mathbf{R_i}|),$$

$$r_i^{-1} \odot n_{bj} = \int d\mathbf{r}' |\mathbf{r}'-\mathbf{r}+\mathbf{R_i}|^{-1} n_b(|\mathbf{r}'-\mathbf{R_j}|).$$

We also define the functional derivative

$$\Delta G'[n+\overline{n}] = \delta G[n+\overline{n}]/\delta n(r),$$

so that the Euler form of the Kohn-Sham equation in the external potential V_{ext} is

$$\Delta G'[n+\overline{n}] - \Delta G'[\overline{n}] + V_{\text{ext}} + r^{-1} \odot n = 0.$$

Thus, for the ion a alone, the above equation becomes

$$\Delta G'[n_{ai}+\overline{n}] - \Delta G'[\overline{n}] - Z_a/r_i + r^{-1} \odot n_{ai} = 0.$$

2. Total pair interaction

The total interaction between the pair of ions a, b immersed in the electron gas can be written as a sum of contributions from the nuclear-nuclear Coulomb interaction $Z_a Z_b/R$, other electrostatic effects Δ_{ES}, and contributions from kinetic energy and exchange-correlations effects $\Delta_{ke+\text{xc}}$. Thus

$$\Psi ab = Z_a Z_b/R + \Delta_{ES} + \Delta_{ke+\text{xc}},$$

$$\Delta_{ke+\text{xc}} = \Delta G[n_{ai}+n_{bj}+\overline{n}] - \Delta G[n_{ai}+\overline{n}] - \Delta G[n_{bj}+\overline{n}],$$

$$\Delta_{ES} = \left[\left\{-\frac{Z_a}{r_i} \otimes n_{bj} + \frac{1}{2} n_a i \otimes \frac{1}{r} \odot n_b j\right\} + \left\{\begin{smallmatrix} a \leftrightarrow b \\ i \leftrightarrow j \end{smallmatrix}\right\}\right].$$

The displaced electron densities n_{ai}, etc., can be written as a sum of a core-electron density c_{ai} and a free-electron density f_{ai}. It is reasonable to assume that the free electron displacement f_{ai} due to the ion is such that, e.g., $f_{ai} \ll c_{ai} + \overline{n}$, etc., everywhere in space. Hence ΔG may be expanded in powers of $f_{i,j} = f_{ai} + f_{bj}$, about the density $c_{i,j} + \overline{n} = c_{ai} + c_{bj} + \overline{n}$, which is a sum of the core electron densities and the density of the uniform electron gas. Thus we have, *formally* to second order,

$$\Delta G[n_{ai}+n_{bj}+\overline{n}] = \Delta G^{(0)} + \Delta G^{(1)} + \Delta G^{(2)},$$

$$\Delta G^{(0)} = \Delta G[c_{i,j}+\overline{n}],$$

$$\Delta G^{(1)} = f_{i,j} \otimes \Delta G'[c_{i,j}+\overline{n}],$$

$$\Delta G^{(2)} = (1/2)(f_{i,j}) \otimes \Delta G''[c_{i,j}+\overline{n}] \otimes (f_{i,j}).$$

At this point it is useful to establish a link with second-order perturbation theory where the bare ionic potential is replaced by a weak pseudopotential w:

$$\left\{-(Z_i/r_i) + \frac{1}{r} \odot c_{ai}\right\} \rightarrow w_{ai}.$$

Further, the pseudopotential approach replaces the $\Delta G'[c_a i + \overline{n}]$ and $\Delta G''[c_a i + \overline{n}]$ type terms by $\Delta G'[\overline{n}]$ and $\Delta G''[\overline{n}]$, leading to the Kohn-Sham equation for the free electron displacement f_{ai}. Thus we have

$$\Delta G''[\overline{n}] \otimes f_{ai} + w_{ai} + \frac{1}{r} \odot f_{ai} = 0$$

and a similar equation for f_{bj}. Hence we have

$$f_{ai} \otimes \Delta G''[\overline{n}] \otimes f_{bj} = \left[-w_{bj} \otimes f_{ai}/2 - f_{ai} \otimes \frac{1}{2r} \odot f_{bj}\right] + \left[\begin{smallmatrix} a \leftrightarrow b \\ i \leftrightarrow j \end{smallmatrix}\right].$$

Using the second-order expansion of $\Delta G[n_{ai}+n_{bj}+\overline{n}]$ in the expression for Ψ_{ab} and using the pseudopotential forms, we get, for the total pair-interaction,

$$\Psi_{ab} = Z_a Z_b/R + \delta G + \Delta\mathcal{E},$$

where

$$\delta G = \Delta G[c_{i,j}+\overline{n}] - \Delta G[c_{ai}+\overline{n}] - \Delta G[c_{bj}+\overline{n}],$$

$$\Delta\mathcal{E} = \frac{1}{2}\left[w_{bj} \otimes f_{ai} - \frac{2Z_a}{r_i} \otimes c_{bj} + c_{bj} \otimes \frac{1}{r} \odot c_{ai}\right] + \frac{1}{2}\left[\begin{smallmatrix} a \leftrightarrow b \\ i \leftrightarrow j \end{smallmatrix}\right].$$

3. Repulsive core-core interaction

The standard metallic interaction in second-order perturbation theory is

$$\phi_{ab} = Z_a^* Z_b^*/R + \frac{1}{2}[w_{bj} \otimes f_{ai} + w_{ai} \otimes f_{bj}].$$

Hence the repulsive interaction is obtained as $\varphi_{ab} = \Psi_{ab} - \phi_{ab}$, with

$$\varphi_{ab} = (Z_a Z_b - Z_a^* Z_b^*)/R + \delta G + \Delta\varphi, \tag{B1}$$

$$\Delta\varphi = \frac{1}{2}\left[-\frac{2Z_a}{r_i} \otimes c_{bj} + c_{bj} \otimes \frac{1}{r} \odot c_{ai}\right] + \left[\begin{smallmatrix} a \leftrightarrow b \\ i \leftrightarrow j \end{smallmatrix}\right].$$

This result still involves the kinetic and exchange-correlation-correction term δG. A more practical form of the core-core repulsion can be obtained as follows. We assume that the core-core repulsion is not sensitive to the details of the functional $G[n]$, in the sense that we can evaluate δG from a *local* functional. A similar method has been described elsewhere [39,40] This means that we can do *local* expansions of the kinetic energy. We divide the space into a left half space (L), containing the ion a, and a right half space (R), containing the ion b, by the perpendicular plane passing through the midpoint of the

bond. In the space (L), the core-electron density c_{bj} is everywhere smaller than $\overline{n}$. Expanding δG, we have

$$\delta G = \int_{(L)} d\mathbf{r} c_{bj}\{\Delta G'[c_{ai}+\overline{n}] - \Delta G'[\overline{n}]\} + \int_{(R)} [{}^{a\leftrightarrow b}_{i\leftrightarrow j}].$$

The core densities are rigid and unaffected by the part of the potential due to the free electrons, so they approximately satisfy a Kohn-Sham equation of the form

$$\Delta G'[c_{ai}+\overline{n}] - \Delta G'[\overline{n}] = -V_{ai},$$

$$-V_{ai} = Z_a/r_i - (1/r) \odot c_{ai}.$$

It follows that

$$\delta G = -c_{ai} \otimes V_{bj} + \int_{(L)} d\mathbf{r}[c_{ai}V_{bj} - c_{bj}V_{ai}].$$

Since the core-electron density c_{ai} is such that

$$c_{ai} = -(4\pi)^{-1}\nabla^2 V_{ai} + Z_a\delta(\mathbf{r}-\mathbf{R_i}),$$

we have

$$\delta G = -c_{ai} \otimes V_{bj} + Z_a V_b(R) + G_I,$$

$$G_I = (4\pi)^{-1}\int_{(L)} d\mathbf{r}[-V_{bj}\nabla^2 V_{ai} + V_{ai}\nabla^2 V_{bj}].$$

The term in $\delta(\mathbf{r}-\mathbf{R_j})$ does not contribute because $\mathbf{R_j}$ is not in the half space (L). The volume integral on the half space can be reduced to a surface integral on the midplane Σ. Then the $\int_{(L)}$ term becomes

$$-(4\pi)^{-1}\int_{\Sigma} d\mathbf{s}[\{V_b dV_a(r)/dr\} + \{a \leftrightarrow b\}].$$

The integrations are now straightforward and we have

$$\delta G = -c_{ai} \otimes V_{bj} + Z_a V_b(R) + (R/4)V_a(R/2)V_b(R/2).$$

Inserting this result into Eq. (B1) gives

$$\phi_{ab} = -(Z_a^* Z_b^*/R) + (R/4)V_a(R/2)V_b(R/2), \qquad \text{(B2)}$$

$$V_a(R) = -(Z_a/R) + \int d\mathbf{r}' c_a(r')/|\mathbf{R}-\mathbf{r}'|$$

and an analogous expression for $V_b(R)$ holds. The behavior of the core-repulsion potential in the small and large R limits is easily verified to be correct. Thus ϕ_{ab} tends to $(Z_aZ_b - Z_a^*Z_b^*)/R$ for $R \to 0$, so that the total interaction Ψ_{ab} reduces correctly to Z_aZ_b/R. For large R, since $V_a(R/2)$ goes to $-2Z_a^*/R$, the repulsive potential is totally screened, as it should be.

APPENDIX C: CONDITION FOR THE EXISTENCE OF Al_n, $n > 1$, MOLECULES

We wish to obtain an estimate of the critical density $n_{\rm crit}$ of the electron gas for which the binding energy of Al_2 becomes zero, at zero temperature. Thus no molecules would exist for $n > n_{\rm crit}$ even at zero temperature. We use a model that, when applied to the embedding of the H_2 molecule [35], was found to give good agreement with more exact calculations. We assume that the electron density effect, i.e., *the change* in the energy $\mathcal{E}$ due to the immersion in the electron gas, with the bond length held fixed at R, is well approximated by the *change* in the model energy $\mathcal{E}_m(R,\overline{n})$ of a suitable "model molecule." This pseudomolecule is an impurity in jellium subject to an external potential that corresponds to the spherical part of the potential of Al_2 around the midpoint of the bond. Thus

$$V_m(r,R) = -2Z^*/(R/2),\ r < R/2\ ,$$
$$V_m(r,R) = -2Z^*/r,\quad r > R/2.$$

Here r is the distance measured from the midpoint of the bond. Thus we write

$$\delta D_m = \mathcal{E}(R,0) - \mathcal{E}(R,\overline{n}) = \mathcal{E}_m(R,0) - \mathcal{E}_m(R,\overline{n}).$$

The spherical symmetry of the model molecule makes it possible to easily evaluate the energy using existing one-center DFT codes, with $Z^* = 3$ for Al. The model is exact for large r but the charge pileup close to the ion centers is not accurately determined. We can correct for this error by adding to $\mathcal{E}_m(R,\overline{n})$ twice the correction (one for each ion of Al_2) that would be produced in the single-atom embedding energy if an external potential $V_m^{(1)} = V_m(r,R)/2$ were used, with half the value of V_m defined previously, since we are now concerned with one ion. Then the required energy correction is $E_a(0,\overline{n}) - E_m^{(1)}(R,\overline{n})$, where $E_a(0,\overline{n})$ is the energy of an Al atom in jellium while $E_m^{(1)}$ is that of a fictitious ion with the external potential $V_m^{(1)}$. Note that $E_a(\infty,0) = E_a(\infty,\overline{n}) = 0$. Thus we can express the change in the binding energy due to immersion of Al_2 in the electron gas as

$$\delta D(R,\overline{n}) = \delta D_m - 2[E_m^{(1)}(R,0) - E_m^{(1)}(R,\overline{n})].$$

We have calculated $\delta D(R,\overline{n})$ at the equilibrium distance of the free molecule for a range of electron densities and found that the binding energy of Al_2 becomes zero at $\overline{n} \simeq 0.0008$ a.u., i.e., for a density $\overline{n} \simeq n_0/32$, where n_0 is the electron density ($r_s = 2.07$ a.u.) of metallic solid aluminum under normal conditions. We conclude that for $n > n_{\rm crit}$, with $n_{\rm crit} = n_0/32$, no molecule formation occurs in Al plasma. For higher temperatures, the binding energy is smaller and hence molecule formation is even less probable.

[1] A. Ng, D. Parfeniuk, P. Celliers, L. Da Silva, R.M. More, and Y.T. Lee, Phys. Rev. Lett. **57**, 1595 (1986).
[2] H.M. Milchberg, R.R. Freeman, S.C. Davey, and R.M. More, Phys. Rev. Lett. **61**, 2364 (1988)
[3] A. Ng, P.Cellier, F. Perrot, M.W.C. Dharma-wardana, R.M. More, Y. H. Lee, and G. Rinker, Phys. Rev. Lett. **72**, 681 (1994).
[4] D. Saumon and G. Chabrier, Phys. Rev. Lett. **62**, 2397 (1989); Phys. Rev. A **46**, 2084 (1992).
[5] F. Hensel, Phys. Scr. **T25**, 283 (1989); R. Redmer and W. W. Warren, Jr., Phys. Rev. B **48**, 14 892 (1993), and references therein.
[6] G. Chabrier and E. Schatzman, in *Equation of State in Astrophysics*, edited by G. Chabrier (Cambridge University Press, Cambridge, 1994).
[7] C. Iglesias and F. Rogers, Science **263**, 50 (1994), discuss opacity calculations for astrophysical plasmas.
[8] M. Saha, Philos. Mag. **20**, 472 (1920).
[9] H.R. Griem, *Spectral Line Broadening by Plasmas* (Academic, New York, 1974).
[10] G.I. Kerley, J. Chem. Phys. **85**, 5228 (1986).
[11] F.J. Rogers, in *High Pressure Equation of State: Theory and Applications*, edited by S. Eliezer and R.A. Ricci (North-Holland, New York, 1991); W. D. Kraeft *et al.*, *Quantum Statistics of Charged Particle Systems* (Plenum, New York, 1986).
[12] J. Christensen-Dalsgaard and W. Däppen, Astron. Astrophys. Rev. **4**, 267 (1993).
[13] D. Mihalas, W. Däppen, and D.G. Hummer, Astrophys. J. **331**, 815 (1988).
[14] D.A. Liberman, Phys. Rev. B **20**, 4981 (1978); R.M. More, K.H. Warren, D.A. Young, and G.B. Zimmerman, Phys. Fluids **31**, 3059 (1988).
[15] B. Rozsnyai, Phys. Rev. A **5**, 1137 (1972).
[16] M.W.C. Dharma-wardana and F. Perrot, Phys. Rev. A **26**, 2096 (1982).
[17] L. Dagens, J. Phys. C **5**, 23 (1972); L. Dagens, J. Phys. F **7**, 1167 (1977); J.M. Ziman, Proc. R. Soc. London **91**, 701 (1967).
[18] F. Perrot, Phys. Rev. A **47**, 570 (1993).
[19] F. Perrot, Phys. Rev. A **42**, 4871 (1990).
[20] N. W. Ashcroft and D. Stroud, Solid State Phys. **33**, 1 (1978).
[21] H. Iyetomi and S. Ichimaru, Phys. Rev. A **34**, 433 (1986); D.G. Kanhere, P.V. Panat, A.K. Rajagopal, and J. Callaway, *ibid.* **33**, 490 (1986); F. Perrot and M.W.C. Dharma-wardana, Phys. Rev. A **30**, 2619 (1984).
[22] N.D. Mermin, Phys. Rev. **137**, A1441 (1965); P. Hohenberg and W. Kohn, *ibid.* **136**, B864 (1964); W. Kohn and L.J. Sham, *ibid.* **140**, A1133 (1965).
[23] (a) M.W.C. Dharma-wardana and F. Perrot, Phys. Rev. Lett. **65**, 76 (1990); (b) F. Perrot and M.W.C. Dharma-wardana, *ibid.* **71**, 797 (1993).
[24] A.C. Maggs and N.W. Ashcroft, Phys. Rev. Lett. **59**, 113 (1987).
[25] L.E. Gonzalez, D.J. Gonzalez, and M. Sibert, Phys. Rev. A **45**, 3803 (1992).
[26] S. Ichimaru and S. Tanaka, Phys. Rev. A **32**, 1790 (1985).
[27] G. Rinker, Phys. Rev. B **31**, 4207 (1985), uses an approach based on the Ziman formula. Other approaches are by R. Cauble and W. Rozmus, Phys. Fluids **28**, 3387 (1985); Y. T. Lee and R. M. More, *ibid.* **27**, 1273 (1984).
[28] R. Evans, B.L. Gyorffy, N. Szabo, and J.M. Ziman, in *Properties of Liquid Metals*, edited by S. Takeuchi (Wiley, New York, 1973).
[29] F. Perrot and M.W.C. Dharma-wardana, Phys. Rev. A **36**, 238 (1987).
[30] M.W.C. Dharma-wardana and F. Perrot, Phys. Rev. A **45**, 5883 (1992).
[31] K.P. Huber and G. Herzberg, *Constants of Diatomic Molecules* (Van Nostrand, New York, 1964).
[32] C.W. Bauschlicher, Jr. and L.G.M. Pettersson, J. Chem. Phys. **87**, 2198 (1987); L.G.M. Pettersson, C.W. Bauschlicher, Jr., and T. Halicioglu, *ibid.* **87**, 2205 (1987).
[33] R.O. Jones, Phys. Rev. Lett. **67**, 22 (1991), and references therein.
[34] J.P. Perdew, H.Q. Tran, and E.D. Smith, Phys. Rev. B **42**, 11 627 (1990).
[35] F. Perrot, J. Phys.: Condens. Matter **6**, 431 (1994).
[36] G.I. Kerley, Sandia Report No. SAND88-2291-UC-405, 1991 (unpublished).
[37] R. M. More, in *Atomic Physics of Highly Ionized Atoms*, edited by R. Marus (Plenum, New York, 1989).
[38] I. Štich, R. Car, and M. Parrinello, Phys. Rev. Lett. **63**, 2240 (1989); G. Galli, R. M. Martin, R. Car, and M. Parinello, *ibid.* **63**, 988 (1989).
[39] F. Perrot and M.W.C. Dharma-wardana, in *Equation of State in Astrophysics* (Ref. [6]).
[40] F. Perrot and N.H. March, Phys. Rev. A **42**, 4884 (1990).